

COMMUNICATION

Facile preparation of nano-micro structure PbSbO_2Cl as a novel anode material for lithium-ion batteries

Cite this: *RSC Advances*, 2013, 3, 372

Received 28th September 2012,

Accepted 13th November 2012

DOI: 10.1039/c2ra22337f

www.rsc.org/advances

Jie Shu,* Rui Ma, Lianyi Shao, Miao Shui, Lu Hou, Kaiqiang Wu, Yuntao Chen, Dongjie Wang, Yunxiao Liang and Yuanlong Ren

We report the development of PbSbO_2Cl as a new anode material for lithium-ion batteries. It is prepared by a simple hydrothermal method from $\text{Pb}(\text{NO}_3)_2$ and SbCl_3 . The as-prepared PbSbO_2Cl shows a well-dispersed nano-micro structure with particle sizes of 200–500 nm. The initial discharge capacity of PbSbO_2Cl is $1011.0 \text{ mAh g}^{-1}$ corresponding to 14.6 Li per formula storage in the structure. In the inverse charge process, a reversible capacity of 731.8 mAh g^{-1} can be delivered. This suggests that PbSbO_2Cl may be a promising high-capacity anode material for lithium-ion batteries.

1. Introduction

Due to their high capacity characteristics, metal oxides have been used worldwide as lithium storage materials since lithium-ion batteries were developed. In the past twenty years, Co, Cu, Mn, and Ni-based transition metal oxides have received more attention than other metal oxides due to their superior lithium storage capabilities.^{1–5} However, high prices inhibit the practical application of these materials in the commercial field of energy storage and conversion. As a result, some cheap lithium storage materials, such as Pb, Sb, Cr, and Fe-based oxides,^{6–14} have been prepared to satisfy the development of lithium-ion batteries. PbO samples, which are prepared by solution techniques, show a reversible capacity of 100 mAh g^{-1} after 50 cycles.^{6,7} After carbon coating, $\text{PbO}@C$ core-shell nanocomposites show improved electrochemical properties with a reversible capacity of 170 mAh g^{-1} after 50 cycles.⁸ This indicates that the present techniques are unsuitable for the development of high capacity Pb-based anode materials.

In recent years, composite oxides, such as CaSnO_3 , CuCrO_2 and CoFe_2O_4 ,^{15–17} have caught the attention of researchers worldwide as a result of their superior cycling ability and high capacity characteristics. In the composite oxides, the different active components react with lithium at different potentials during the

charge and discharge processes. As a result, the other components can act as buffers to relieve the volume change of the sample when one component is reacting with lithium. Most recently, transition metal chlorides, such as CoCl_2 , AgCl and CuCl_2 ,^{18,19} have been used as lithium storage materials for lithium-ion batteries. They show excellent cycling capability and high reversible capacity. It has also been found that there are quite different electrochemical working plateaus between chlorides and oxides. Therefore, it can be expected that metal oxide chlorides will exhibit superior electrochemical performance due to their composite structures.

In this paper, a novel lithium storage material (PbSbO_2Cl) is reported. It is prepared by a simple hydrothermal method. The structure and morphology are described by XRD, FTIR, SEM and HRTEM. The electrochemical results show that PbSbO_2Cl is a potential anode candidate for lithium-ion batteries.

2. Experimental section

PbSbO_2Cl is obtained by using $\text{Pb}(\text{NO}_3)_2$ and SbCl_3 as the starting materials. Firstly, $\text{Pb}(\text{NO}_3)_2$ and SbCl_3 are dissolved in distilled water. Then, the Pb^{2+} and Sb^{2+} in the solution are totally deposited by the $\text{NH}_3\cdot\text{H}_2\text{O}$. After that, the mixed solution including the obtained white intermediate are put into a Teflon-lined stainless steel autoclave and maintained at $160 \text{ }^\circ\text{C}$ for 24 h. Finally, the resulting product is filtered and washed by distilled water and ethanol, then dried at $100 \text{ }^\circ\text{C}$ for 24 h. All chemical reagents in the experiment were purchased from Sinopharm Chemical Reagent Shanghai Co. Ltd in China.

The X-ray diffraction (XRD) phase patterns for the intermediate and resulting samples were recorded by a Bruker D8 Focus diffractometer using nickel-filtered $\text{Cu-K}\alpha$ radiation. Fourier transform infrared (FTIR) spectra were collected by a Shimadzu infrared spectrophotometer at wavenumbers between 400 and 1000 cm^{-1} . The surface morphology of as-prepared samples was characterized by a Hitachi scanning electron microscope (SEM). The fine grain structure of PbSbO_2Cl was observed with a JEOL high resolution transmission electron microscope (HRTEM).

PbSbO_2Cl working electrode was fabricated by using the resulting powder (80 wt.%), carbon black (10 wt.%) and

Faculty of Materials Science and Chemical Engineering, Ningbo University, Ningbo 315211, Zhejiang Province, People's Republic of China.

E-mail: sergio_shu@hotmail.com; shujie@nbn.edu.cn; Fax: +86-574-87609987;

Tel: +86-574-87600787

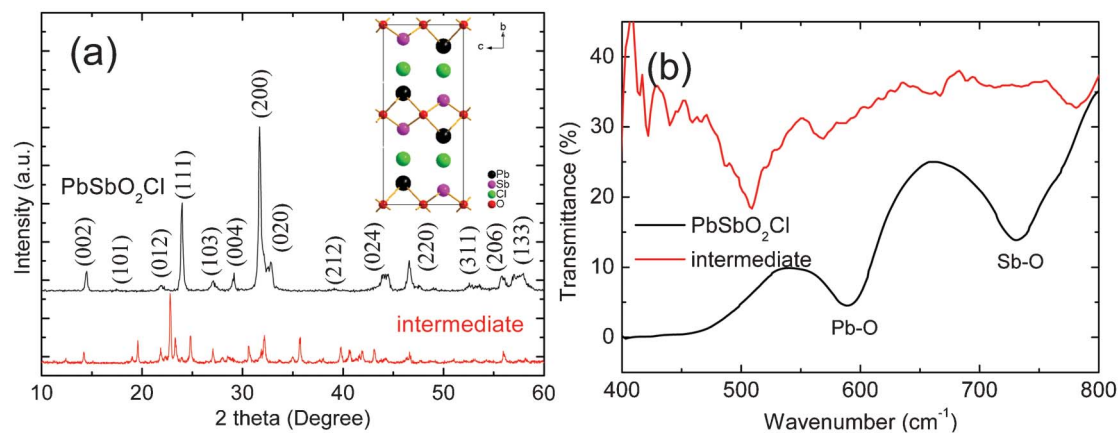


Fig. 1 XRD (a) and FTIR (b) patterns of PbSbO_2Cl and its intermediate.

polyvinylidene fluoride (10 wt.%) as starting materials. A homogeneous slurry can be formed by adding *N*-methylpyrrolidine into the mixture. The testing electrode was prepared by casting the slurry on a copper foil and drying at 120 °C for 12 h in a vacuum oven, then cut into discs with a diameter of 15 mm.

$\text{PbSbO}_2\text{Cl}/\text{Li}$ battery was assembled by using PbSbO_2Cl film as cathode, Whatman glass fiber filter as separator, metal lithium disc as anode and 1 mol L^{-1} LiPF_6 dissolved in a mixture of ethylene carbonate and dimethyl carbonate (1 : 1, v/v) as the electrolyte in an Etelux Ar-filled glove box. All the charge/discharge cycles were recorded on a multi-channel Land battery testing system in a constant temperature cabinet (25 °C). Cyclic

voltammograms (CV) and electrochemical impedance spectra (EIS) of the $\text{PbSbO}_2\text{Cl}/\text{Li}$ battery were collected on a CHI 660D electrochemical working station in the frequency range between 100 000 and 0.01 Hz with an amplitude of 5 mV.

3. Results and discussion

Fig. 1a and 1b show the XRD and FTIR patterns of the intermediate and resulting samples. Based on the JCPDS cards, the intermediate obtained from the deposition of $\text{Pb}(\text{NO}_3)_2$ and SbCl_3 mixed solution is a mixed material composed of unknown and known compounds, such as $\text{Pb}(\text{OH})_2$. After hydrothermal

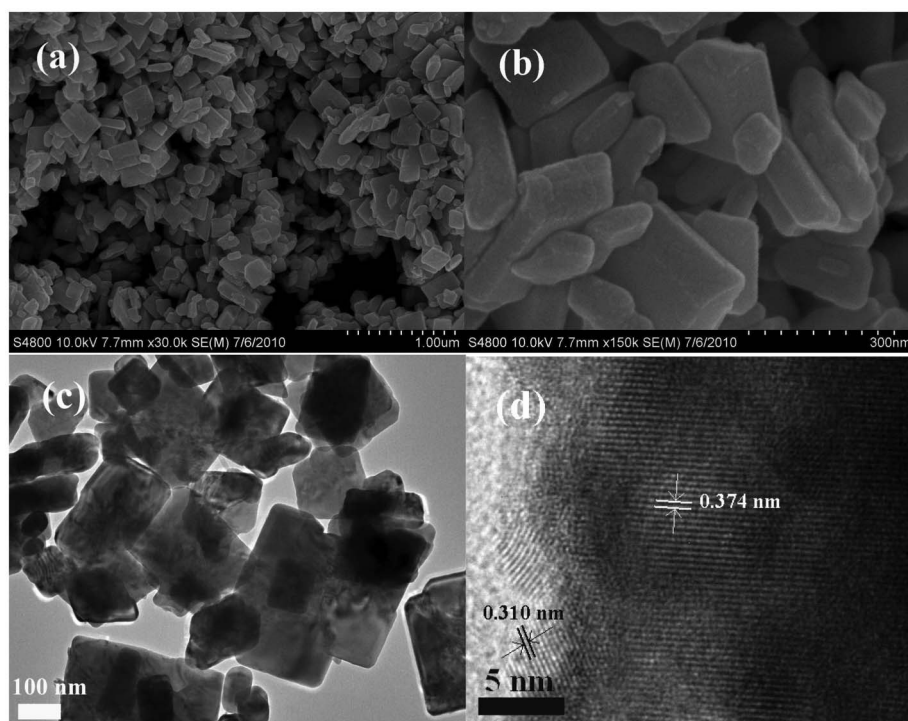


Fig. 2 SEM (a,b), TEM (c) and HRTEM (d) images of PbSbO_2Cl .

reaction, PbSbO_2Cl phase is formed as described by the XRD pattern. The main diffraction peaks located at 14.5° , 24.0° , 31.7° , 32.9° , 44.1° and 46.6° correspond to the (002), (111), (200), (020), (204) and (220) planes. It is attributed to the JCPDS card No.17-0469, namely the PbSbO_2Cl phase. As shown in Fig. 1a, the unit cell of PbSbO_2Cl is orthorhombic, space group Bmmb (No. 63). The refined unit cell parameters are $a = 5.601$, $b = 5.429$ and $c = 12.189$ Å by using Fullprof software. The structure of PbSbO_2Cl consists of sheets of $[\text{PbO}_{4/4}]^0$ and $[\text{SbO}_{4/4}]^+$ cations, which are separated by Cl^- . As a result of the stereoactive lone pairs, both Pb^{2+} and Sb^{3+} cations are in asymmetric coordination environments. As seen from the FTIR spectra in Fig. 1b, the featured bands for PbSbO_2Cl at 589 and 732 cm^{-1} can be assigned to the stretching vibrations of Pb–O and Sb–O bonds, respectively. This is consistent with the previous results reported by Y. Porter.²⁰

Fig. 2 shows the SEM, TEM and HRTEM images of PbSbO_2Cl . As shown in Fig. 2a and 2c, the as-prepared PbSbO_2Cl powders are well-dispersed nano-micro structures with particle sizes of 200–500 nm. Therefore, they are suitable as a powder anode material for lithium-ion batteries. As the HRTEM images show in Fig. 2d, the lattice distances are measured to be 0.374 and 0.310 nm, which correspond to the featured (111) and (004) planes of the as-prepared PbSbO_2Cl sample, respectively. This is consistent with the XRD result shown in Fig. 1a.

Fig. 3a shows CVs of the PbSbO_2Cl lithium storage material. There are seven reduction peaks at 2.28, 1.76, 1.69, 1.13, 0.70, 0.40, 0.19 V and six oxidation peaks at 0.56, 0.67, 1.10, 1.36, 1.98, 2.34 V in the initial cycle. The appearance of so many redox peaks is attributed to the complex electrochemical lithiation process to form Li_xSb , Li_yPb , Li_2O and LiCl . The asymmetric behavior of reduction and oxidation peaks shows the irreversible reactions between PbSbO_2Cl and lithium. In the subsequent scans, the shape and position of reduction and oxidation peaks are similar to each other except for the peak currents and some irreversible peaks in the high potential range (>1.5 V). This indicates that the deterioration of PbSbO_2Cl as a lithium storage material in the range 0.0–3.0 V mainly results from the irreversible behavior in the initial cycles. The electrochemical cycles of PbSbO_2Cl are shown in Fig. 3b. There are several lithiated and delithiated plateaus appearing in the charge/discharge cycles, which correspond to the reduction and oxidation peaks in CVs. The first discharge and charge capacities of PbSbO_2Cl are 1011.0 and 731.8 mAh g^{-1} , respectively. Based on the reaction of PbSbO_2Cl with Li to form $\text{Li}_{4.4}\text{Pb}$, Li_3Sb , Li_2O and LiCl , it is known that the theoretical capacity of PbSbO_2Cl is 838.6 mAh g^{-1} . The extra capacity (172.4 mAh g^{-1}) is probably attributed to the irreversible electrolyte decomposition to form a solid electrolyte interphase film. At the second

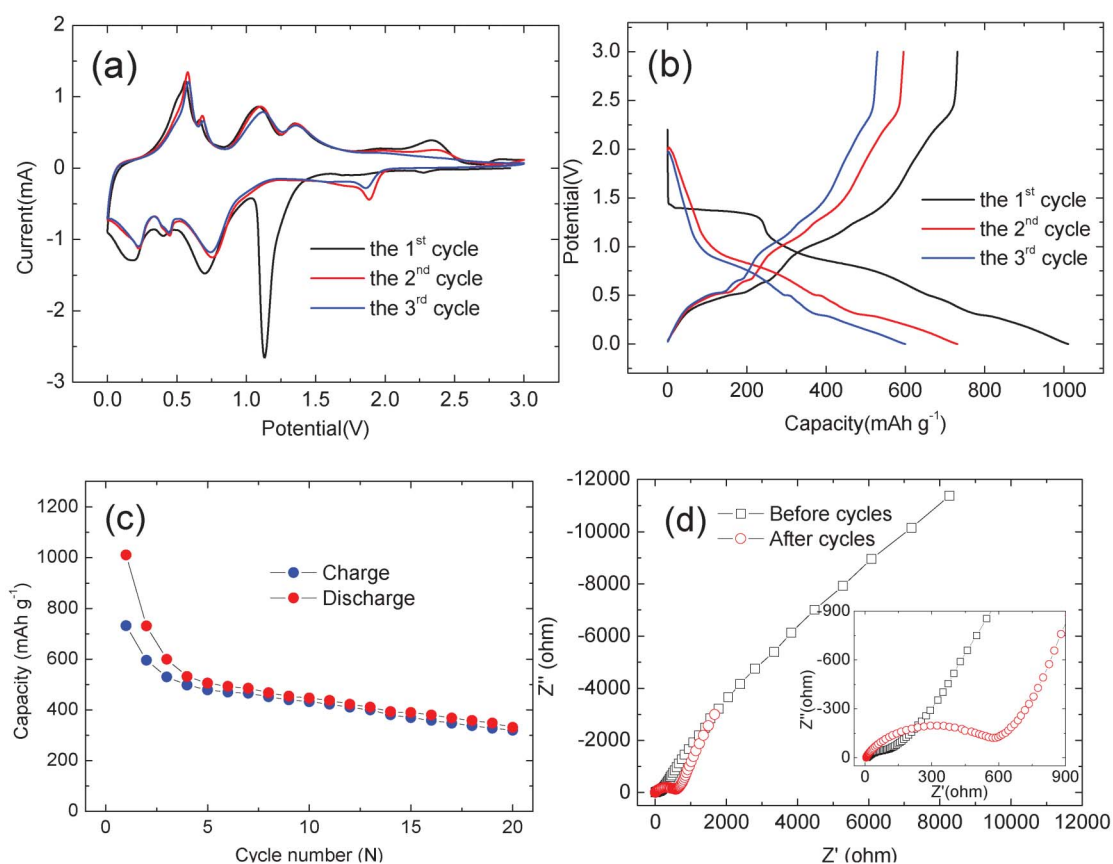


Fig. 3 CVs (a), charge/discharge curves (b), cycling properties (c) and EIS (d) spectra of PbSbO_2Cl .

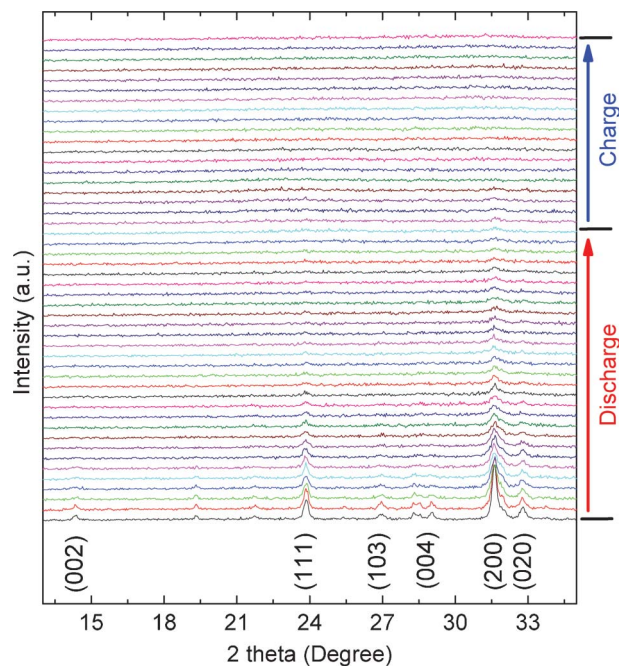


Fig. 4 *In situ* XRD patterns of PbSbO₂Cl cycled in 0.0–3.0 V.

cycle, the discharge and charge capacities of PbSbO₂Cl are 731.2 and 595.7 mAh g⁻¹, respectively. As shown in Fig. 3b, the decrease of reversible lithium storage capacity in the initial two cycles is mainly attributed to the disappearance of lithiated plateau at 1.38 V. After twenty cycles, the reversible discharge and charge capacities of PbSbO₂Cl as shown in Fig. 3c are 330.7 and 319.4 mAh g⁻¹, respectively. Based on calculation, it is known that the capacity retention is merely 43.5%. It suggests that there is a huge irreversible capacity during the electrochemical cycles. It also indicates that pure PbSbO₂Cl has some disadvantages as a lithium storage material for lithium-ion batteries. To study the capacity loss, the EIS spectra are shown in Fig. 3d before and after cycles. It is found that the impedance of the electrode increases after the electrochemical cycles. As reported,^{1,21} this always comes from the structure changes of the power electrode. To investigate the effect of structural evolution on the cycling properties, *in situ* studies were performed on the initial cycle of PbSbO₂Cl. As the *in situ* XRD results show in Fig. 4, the featured diffraction peaks for PbSbO₂Cl gradually disappear with the increase of lithium content in the structure. In the charge process, the compound maintains an amorphous state as no diffraction peak reappeared in the XRD patterns. These phenomena are similar with the structural changes of oxides or fluorides during their electrochemical cycles.^{19,22} It indicates that the breakdown of structure and pulverization of nano-micro structured bulks should be responsible for the impedance increase and capacity loss of PbSbO₂Cl. Therefore, carbon coating may be a favorable way to maintain the crystal structure and improve the cycling properties of PbSbO₂Cl in future work.

4. Conclusions

In this paper, PbSbO₂Cl is studied as an anode material for lithium-ion batteries. The preparation of PbSbO₂Cl is accomplished by the hydrothermal reaction of Pb(NO₃)₂ with SbCl₃ in a NH₃·H₂O saturated solution. The well-dispersed samples are light yellow nano-micro structures with particle sizes of 200–500 nm. Upon use as a lithium storage material, the initial discharge and charge capacities of PbSbO₂Cl are 1011.0 and 731.8 mAh g⁻¹, respectively. After twenty cycles, the reversible discharge and charge capacities of PbSbO₂Cl can be maintained at 330.7 and 319.4 mAh g⁻¹, respectively. *In situ* XRD results show that the breakdown of the structure may be responsible for the capacity loss of PbSbO₂Cl during cycles.

Acknowledgements

This project is sponsored by National Science Foundation of China (No. 51104092), Key Project of Chinese Ministry of Education (No. 210083), Qianjiang Talent Project of Zhejiang Province (2011R10089) and the Open Project of Key Lab Adv Energy Mat Chem (Nankai Univ) (KLAEMC-OP201201). The work is also supported by the K. C. Wong Magna Fund in Ningbo University.

References

- P. Poizot, S. Laurelle, S. Grugeon, L. Dupont and J. M. Tarascon, *Nature*, 2000, **407**, 496–499.
- H. Liu, G. X. Wang, J. Liu, S. Z. Qiao and H. J. Ahn, *J. Mater. Chem.*, 2011, **21**, 3046–3052.
- X. H. Huang, J. P. Tu, C. Q. Zhang, X. T. Chen, Y. F. Yuan and H. M. Wu, *Electrochim. Acta*, 2007, **52**, 4177–4181.
- H. Xia, M. O. Lai and L. Lu, *J. Mater. Chem.*, 2010, **20**, 6896–6902.
- B. Wang, X. L. Wu, C. Y. Shu, Y. G. Guo and C. R. Wang, *J. Mater. Chem.*, 2010, **20**, 10661–10664.
- K. Konstantinov, S. H. Ng, J. Z. Wang, G. X. Wang, D. Wexler and H. K. Liu, *J. Power Sources*, 2006, **159**, 241–244.
- S. H. Ng, J. Wang, K. Konstantinov, D. Wexler, J. Chen and H. K. Liu, *J. Electrochem. Soc.*, 2006, **153**, A787–A793.
- Q. M. Pan, Z. J. Wang, J. Liu, G. P. Yin and M. Gu, *Electrochem. Commun.*, 2009, **11**, 917–920.
- H. Bryngelsson, J. Eskhult, L. Nyholm, M. Herranen, O. Alm and K. Edstrom, *Chem. Mater.*, 2007, **19**, 1170–1180.
- M. Z. Xue and Z. W. Fu, *Electrochem. Commun.*, 2006, **8**, 1250–1256.
- L. Y. Jiang, S. Xin, X. L. Wu, H. Li, Y. G. Guo and L. J. Wan, *J. Mater. Chem.*, 2010, **20**, 7565–7569.
- B. K. Guo, M. F. Chi, X. G. Sun and S. Dai, *J. Power Sources*, 2012, **205**, 495–499.
- M. V. Reddy, T. Yu, C. H. Sow, Z. X. Shen, C. T. Lim, G. V. Subba Rao and B. V. R. Chowdari, *Adv. Funct. Mater.*, 2007, **17**, 2792–2799.
- H. S. Lim, B. Y. Jung, Y. K. Sun and K. D. Suh, *Electrochim. Acta*, 2012, **75**, 123–130.
- Y. Sharma, N. Sharma, G. V. Subba Rao and B. V. R. Chowdari, *Chem. Mater.*, 2008, **20**, 6829–6839.
- J. Shu, X. D. Zhu and T. F. Yi, *Electrochim. Acta*, 2009, **54**, 2795–2799.

- 17 P. Lavela, J. L. Tirado, M. Womes and J. C. Jumas, *J. Electrochem. Soc.*, 2009, **156**, A589–A594.
- 18 T. Li, Z. X. Chen, Y. L. Cao, X. P. Ai and H. X. Yang, *Electrochim. Acta*, 2012, **68**, 202–205.
- 19 J. L. Liu, W. J. Cui, C. X. Wang and Y. Y. Xia, *Electrochem. Commun.*, 2011, **13**, 269–271.
- 20 Y. Porter and P. S. Halasyamani, *Z. Naturforsch.*, 2002, **57b**, 360–361.
- 21 H. Li, L. H. Shi, W. Lu, X. J. Huang and L. Q. Chen, *J. Electrochem. Soc.*, 2001, **148**, A915–A922.
- 22 J. Hu, H. Li and X. J. Huang, *Electrochem. Solid-State Lett.*, 2005, **8**, A66–A69.